(NASA-TM86179) SOLAR He-3-RICH EVENTS AND NON-RELATIVISTIC ELECTRON EVENTS: A NEW ASSOCIATION (NASA) 27 p HC A03/MF A01
CSCL 03B
N85-15652
Unclas
G3/92 13037

NASA

Technical Memorandum 86179

SOLAR ^{3}HE-RICH EVENTS AND NON-RELATIVISTIC ELECTRON EVENTS: A NEW ASSOCIATION

D. V. REAMES, T. T. VON ROSENVINGE, AND R. P. LIN

NOVEMBER 1984

National Aeronautics and Space Administration

Goddard Space Flight Center
Greenbelt, Maryland 20771

SOLAR ^{3}HE-RICH EVENTS AND NON-RELATIVISTIC ELECTRON EVENTS: A NEW ASSOCIATION*

D. V. Reames and T. T. von Rosenvinge
NASA/Goddard Space Flight Center, Greenbelt, MD 20771

and

R. P. Lin
Space Sciences Laboratory, University of California, Berkeley, Berkeley, CA 94720

ABSTRACT

In 15 months of observation by the ISEE-3 spacecraft, we find that virtually all solar $\gtrsim$ 1.3 MeV/nucleon ^{3}He-rich events are associated with impulsive 2 to ~ 10^2 keV electron events, although many electron events were not accompanied by detectable ^{3}He increases. Both the ^{3}He and the electrons exhibit nearly scatter-free propagation in the interplanetary medium, and the times of onset and maximum for the ^{3}He and electron increases are closely related by velocity dispersion. The electron events and their related type III solar radio bursts provide, for the first time, identification of the flares which produce ^{3}He-rich events. ^{3}He appears to be accelerated at the flash phase of solar flares along with nonrelativistic electrons

*Accepted for Publication in the Astrophysical Journal

I. INTRODUCTION

Solar ^{3}He-rich events represent one of the most striking composition anomalies among the observed populations of solar and interplanetary energetic particles. From the earliest observations (Schaffer and Zahringer, 1962; Hseih and Simpson, 1970; Anglin et al., 1973; Dietrich, 1973; Garrard et al., 1973), events were found to have ratios of the neighboring isotopes, ^{3}He/^{4}He, of order unity, while the typical ratios for the solar atmosphere or solar wind are a few times 10^{-4} (Geiss and Reeves, 1972). While the ^{3}He/^{4}He ratio in the solar wind varies, it remains below 10^{-2}, and the enhanced ratios are not correlated with the occurrence of solar ^{3}He-rich events (Coplan et al., 1983). Other properties of ^{3}He-rich events (reviewed by Ramaty et al., 1980) include reduced ^{1}H/^{4}He ratios and enhanced abundances of Fe and other heavy elements, and a tendency to larger ^{3}He enhancements in smaller events

While most observers have studied the events on an event-averaged basis, Reames and von Rosenvinge (1983), using the high sensitivity ISEE-3 measurements, were able to study the ^{3}He time histories and angular distributions during individual events. They found that ^{3}He events exhibited: (a) fast temporal behavior and velocity dispersion, (b) magnetic-field-aligned flows with the ^{3}He particles streaming away from the Sun during most of the event, and (c) the presence of ~ 300 keV electrons during many of the events.

Non-relativistic, ~ 10-10^2keV solar electron events (Van Allen and Krimigis, 1965; Anderson and Lin, 1966; Lin and Anderson, 1967; Lin 1970) are the most frequent of solar energetic-particle emissions. Their properties, reviewed by Lin (1974), include frequent propagation of the electrons in an almost scatter-free mode through the interplanetary medium and close association with Type III solar radio bursts, X-ray bursts, and the flash phase of solar flares (Lin et al., 1981). The 2-10^2 keV electrons appear responsible for the generation of type III radio emission in the interplanetary plasma. More recently, Potter, Lin, and Anderson (1980) showed that below ~ 10 keV electron events occurred even more frequently than above 10 keV, and that essentially all of the 2-10 keV events exhibited scatter free propagation.

The ability to correlate ^{3}He and electron events requires relatively high time resolution since the electron events often occur at rates of several per day. If the rise times for low-energy nuclei were 1-2 days, as is often the case in large flares, correlations would be almost impossible.

II. INSTRUMENTATION

Particle measurements described in this paper were made aboard the ISEE-3 spacecraft located in halo orbit about the libration point, ~ 240 Earth radii upstream of Earth in the Sunward direction. Our study covers measurements made during the time period from shortly after launch on August 12, 1978 through November 21, 1979.

Helium isotope data were obtained using the Very Low Energy Telescope (VLET) on the medium-energy cosmic-ray experiment described by von Rosenvinge et al. (1978). The telescope covers energies above 1.3 MeV/nucleon for ^{3}He with two thin (15μ) solid state detectors followed by a third 320 μ element and a 320 μ anticoincidence element. Owing to the relatively small size of the ^{3}He-rich events and to their steep spectra, the statistically best measurements are obtained for the lowest energy particles which stop in the second 15 μ element. Figure 1 shows a plot of dE/dx versus E for this lowest-energy region and demonstrates the degree of isotope resolution obtained.

The ^3He-rich event periods studied here have been previously identified in a scan of VLET data, subject to criteria described by Reames and von Rosenvinge (1983). This scan selected times when two or more consecutive 6-hour averaging periods each had $^3He/^4He > 0.20$ and each had errors in the ^3He intensity of < 50 percent. A list of these event periods is given in Kahler et al. (1984b).

The electron data were obtained with the University of California experiment on the same spacecraft (Anderson et al., 1978). This experiment consists of an electrostatic analyzer for observing 2 to 10 keV electrons and semiconductor detector telescopes for detecting electrons from 15 keV to 1 MeV. Over 300 impulsive electron events were identified in the period of observations.

III. RESULTS

A) Time Correlations

The May 17, 1979 event shown in Figure 2 is the largest ^3He event in during the study period and hence permits the most complete analysis. The higher energy (> 19 keV) channels for the electrons show sporadic contamination by particles flowing upstream from the Earth's bow shock; for example, near 0400, 1300, and $\gtrsim$ 1500 UT. Also some increases due to solar X-rays were observed in the 53-104 keV channel at ~ 0230 and after 1700 UT. Despite this background in the electron data, velocity dispersion, with particle arrival times varying inversely with their velocity, can be seen separately in the ^3He and electron data for this event at 0558 UT.

Figures 3 and 4 show examples of the multiple events that occur frequently in the data. These "storms" of electron events from a single active region (Lin, 1971) often appear to be accompanied by ^3He increases. The larger electron increases at 1330 UT and 2140 UT on December 26, 1978 shown in Figure 3 are accompanied by corresponding increases in ^3He, but the smaller electron events earlier in the day do not produce measurable ^3He. Each of the larger electron increases in the group on September 6, 1979, shown in Figure 4, appears to contribute ^3He but resolution of the individual ^3He increases is difficult.

The final example in Figure 5 shows a relatively large electron increase accompanied by a smaller, more slowly evolving ^3He event.

A more detailed look at the timing is provided by the velocity dispersion plot in Figure 6. Here we have plotted the arrival times, t, of the particles versus $1/\beta$, where the particle velocity is $v = \beta c$. If all the particles were released at the same time, t_0, and traveled the same distance, L, their arrival times would be related by $t=t_0 + L/\beta c$, which would be a straight line on Figure 6. For each interval of inverse velocity, the times of onset and maximum of particle flux are plotted in the figures. For some ^3He channels where statistics are more limited, a single point covers the time of maximum. It should be noted, of course, that the observed time of onset depends upon the relative instrument sensitivity, the rise time, and the event amplitude. From Figure 6 one sees that the ^3He onsets lag the time that would be expected from the electron measurements by no more than about 10-15 minutes. The traversal distance implied by the onset time of the lowest velocity ^3He is ~ 1.3 AU. This compares with ~ 1.25 AU for the electrons.

The times of maximum of ^3He are also consistently later than those of electrons of the same velocity implying a greater degree of scattering for ^3He in the interplanetary medium. The magnetic rigidity of the ^3He is a factor of 2750 greater than that of electrons of the same velocity, hence the ^3He should be scattered by comparably larger-scale irregularities in the interplanetary field. The mean path length implied by the ^3He times of maximum are ~ 1.8-2.0 AU compared to ~ 1.45 AU for the electrons.

B) Event Association and Statistics

A list of events for which electron-^3He correlations have been made are given in Table I. All of the events in Table I are accompanied by metric type III radio bursts, and most by soft X-ray bursts and Hα flares. The optical and radio data in Table I were obtained from Solar-Geophysical Data with the exception of those observed at Big Bear Solar Observatory which were kindly provided by M. Liggett (private communication). The soft X-ray data are from the ISEE-3 solar X-ray experiment (S. R. Kane, private communication). The ^3He electron associated events almost all come from flares located in the western hemisphere of the Sun, near the footpoint (~ W 55 for nominal 400 km/sec solar wind velocity) of the spiral interplanetary field line passing near the Earth. All the associated H_α activity consists of subflares, and the soft X-ray bursts are generally small. Where multiple events occur in a day, the associated flares come from a single active region.

There are many more ^3He enhancements where the poor statistics of the ^3He measurements preclude the identification of individual electron--^3He events. Impulsive electron events accompany all ^3He-rich event periods where data are available even when individual ^3He increases can not be identified.

The inverse correlation is not complete however. There are many examples of large clear electron events that are not accompanied by ^3He. Whether this arises because of limited sensitivity of the ^3He detector or for more fundamental reasons is not known.

C) Other Properties of the Events

We next explore other properties of these events by a detailed case study of the May 17, 1979 event. This event is dominated by ^{3}He; as shown in Figure 7, there is no measurable increase in ^{4}He above pre-existing background from an earlier event. Even without background subtraction, we find ^{3}He/^{4}He $\gtrsim$ 10 and ^{3}He/H $\gtrsim$ 1 at 1 MeV/nucleon near event maximum.

Event integrated angular distributions of He and electrons are shown in Figure 8 and 9, respectively. The ^{3}He distribution is sectored about the Sun-Earth line while the electrons are sectored about the magnetic field direction. The magnetic field remained within ~ 20° of the anti-solar direction through this period.

The distributions show the strong field-aligned flows consistent with the minimal scattering deduced from the time histories. The distribution for ^{3}He is seen to be broader than those of the electrons (despite coarser sectoring) implying more interplanetary scattering consistent with the longer propagation times observed for ^{3}He.

Energy spectra for the two species are shown in Figure 10 together with least-squares fits to a power-law spectral form. The spectral indices of these fits are 2.7 ± 0.1 and 2.7 ± 0.3 for electrons and ^{3}He, respectively. For electrons, only the region from 2.3 to 60 keV was fit because of apparent spectral changes at higher and lower energies. We note that ^{3}He and electrons have the same spectral slope over ranges of comparable particle velocities.

IV. DISCUSSION

The primary result of this work is the establishment of a clear association between the ^{3}He-rich events and the non-relativistic solar electron events. This association is not probablistic in nature but depends upon the close relationship of the arrival times of the particles of different velocity.

Particle acceleration in solar flares has generally been discussed in terms of two phases (e.g., Ramaty et al., 1980; Forman et al., 1982) in the flash phase the 10-100 keV electrons are accelerated. Electrons moving downward into higher density material produce X-rays by bremsstrahlung and those escaping upward produce Type III radio emission by excitation of the local plasma of increasingly lower density. A second phase occurs in some events to accelerate energetic ions, perhaps by passage of shock through the solar atmosphere accompanied by type II and type IV radio emissions and coronal mass ejections with which the energetic proton events are well correlated (Kahler et al., 1983). Recent solar gamma-ray measurements, however, indicate that proton acceleration may on occasion occur simultaneously with the impulsive first phase (Forrest et al., 1981). Although γ-ray events are poorly correlated with the observation of protons in space (Cliver et al., 1983), it is probable that ion acceleration occurs both in the impulsive phase of events and in the ensuing shock.

Electron observations at 1 A.U. indicate two distinct classes of energetic solar particle events, those which accelerate nonrelativistic electrons without any $\gtrsim$ 10 MeV ions detectable above background, and those which accelerate both $\gtrsim$ 10 MeV ions and electrons up to relativistic energies

(Lin, 1974). The nonrelativistic electron events typically arise from small flares or subflares accompanied by Type III radio emission.

Within this picture the ^{3}He-rich events now become associated with flash-phase, nonrelativistic-electron acceleration.

This association of ^{3}He with first-phase acceleration is further supported by Kahler et al. (1984b) who find that ^{3}He events, unlike proton events, are not associated with either Type II radio emission or with coronal mass ejections.

A second result from the electron-^{3}He study relates to their propagation. The short propagation path length for both electrons and ions in ^{3}He-rich events suggests that nearly scatter-free conditions must exist over a wide range of particle gyroradius much of the time. Since ^{3}He rich events are substantially lower in flux than normal solar cosmic ray events, it may be that they can only be observed when propagation and escape conditions are favorable. The association of many of the ^{3}He rich events with storms of electron events may just be the result of such favorable interplanetary propagation and solar escape conditions.

The currently accepted model for ^{3}He enhancement (Fisk, 1978) involves preferential heating of ^{3}He by resonance absorption of ion cyclotron waves created by a common current instability. This model requires, among other things, that the electron temperature be less than 10 times the ion temperature in the ^{3}He injection region. This preferential heating provides enhanced ^{3}He injection for subsequent acceleration to the energies which are observed in interplanetary space. The fact that the ^{3}He and electron spectral slopes are the same at approximately the same particle velocities suggests that the acceleration is velocity dependent. A similar conclusion was inferred by Lin, Mewaldt and Van Hollebeke (1982), in comparing electron and proton spectra in large flare events.

TABLE I

ELECTRON--^{3}He EVENTS

Date	H_α Onset	Flare Location		Type III	Soft X-ray	Onset e-	Onset ^{3}He	^{3}He/^{4}He
1978 Nov. 8	1751	N18E12 McM643	1B	1751	1753	1805	2130	0.36 ± 0.10
Nov. 27	2055	N26W47* McM672	-B	2056	2058	2115	0030	$26.0^{+\infty}_{-10.}$
Dec. 26		N/A		1319	1323	1330	1600	3.1 ± 0.6
Dec. 26	2104	S21W48* McM721	-F	2111 2122	2119 2125	2140	0000	0.8 ± 0.2
1979 Feb. 10	1817	N12W90* McM802	-N	1818	N/A	1835	2300	0.68 ± 0.10
May 17		N/A		0558	None	0610	0900	$12.0^{+\infty}_{-2.0}$
Aug. 14	1728	S18W45 McM205	-N	1728	1730 1735	1738	2000	≲ 0.03
Aug. 14	2048	S17W48 McM205	-B	2048	2050 2053	2100	2330	0.12 ± 0.02
Sept. 6	0906	N20W62 McM252	-F	0906	0908	>0920 <0950	1200	$2.0^{+2.3}_{-1.4}$
Sept. 6	1148	N18W67 McM252	-F	1148	1148	1200	1400	$2.4^{+2.8}_{-1.7}$
Sept. 6	1332	N16W63 McM252	-N	1332	1335 1337	1355	1700	0.26 ± 0.10
Sept. 6	1850	N16W65* McM252	-F	1852	1854	1925	2130	0.44 ± 0.10

* From Big Bear Observatory, based on comments by M. Liggett

ACKNOWLEDGEMENTS

We wish to thank S. Kahler for his assistance with the flare identifications and we are especially grateful to M. Liggett for providing unpublished data on H_α events. The research at the University of California, Berkeley was supported in part by NASA Grant NAG 5-376.

REFERENCES

Anderson, K. A. and Lin, R. P., Phys. Rev. Letters 16, 1121, 1966.

Anderson, K. A., Lin, R. P., Potter, D. W., and Heetderks, H. D., IEEE Transactions on Geoscience Electronics GE-16, 153, 1978.

Anglin, J. D., Dietrich, W. F., and Simpson, J. A., High Energy Phenomena on the Sun, R. Ramaty and R. G. Stone (Eds.), NASA SP-342, 315, 1973.

Cliver, E. W., Forrest D. J., McGuire, R. E., and von Rosenvinge, T. T., 18th International Cosmic Ray Conf., Bangalore, India, Conference Papers 4, 84 (1983).

Coplan, M. A., Ogilvie, K. W., Boschsler, P., and Geiss, J., Solar Wind Five, NASA CP2280, 591, 1983.

Dietrich, W. F., Ap. J. 180, 955, 1973.

Fisk, L. A., Ap. J. 224, 1048, 1978.

Forman, M. A., Ramaty, R., and Zweibel, E. G., The Physics of the Sun, Chapter II, Holzer, T. E., Micholos D., Sturrock, P. A., and Ulrich R. K. (Eds.), 1982

Forrest, D. J., Chupp, E. L., Ryan, J. M., Reppin, C., Riegler, E., Kanbach, G., Pinkau, K., Share, G., Kinzer, G., 17th International Cosmic Ray Conf., Paris, France, Conference Papers 10, 5 (1981).

Garrard, T. L., Stone, E. C., and Vogt, R. F., High Energy Phenomena on the Sun R. Ramaty and R. G. Stone (Eds.), NASA SP-342, 341, 1973.

Geiss, J. and Reeves, H., Astronomy Astrophys. 18, 126, 1972.

Hseih, K. C. and Simpson, J. A., Ap. J. Letters 162, L191, 1970.

Kahler, S. W., Sheeley, N. R., Jr., Howard, R. A., Koomen, M. J., Michels, D. J., McGuire, R. E., von Rosenvinge, T. T., and Reames, D. V.. J. Geophys. Res. (in press), 1984

Kahler, S. W., Reames, D. V., Sheeley, N. R., Jr., Howard, R. A., Koomen, M. J., and Michels, D. J., Astrophys. J. (to be published) 1984b.

Lin, R. P. and Anderson, K. A., Solar Physics 1, 446, 1967.

Lin, R. P., Solar Physics 12, 209, 1970.

Lin, R. P., Solar Physics 15, 453, 1971.

Lin, R. P., Space Science Reviews 16, 189, 1974.

Lin, R. P., Potter, D. W., Gurnett, D. A., and Scarf, F. L., Ap. J., 251, 364, 1981.

Lin, R. P., Mewaldt, R. A., and Van Hollebeke, M. A. I., Ap. J. 253, 949, 1982.

Potter, D. W., Lin, R. P., and Anderson, K. A., Ap. J. Lett 236, L97, 1980.

Ramaty, R., Colgate, S. A., Dulk, G. A. Hoyng, P., Knight, J. W., Lin, R. P. Melrose, D. B., Orrall, F., Shapiro, P. R., Smith, D. F., and Van Hollebeke, M., Solar Flares, A. Monograph from the Skylab Solar Workshop II, P. A. Sturrock, (Ed.), Colorado Assoc. University Press, 117, 1980.

Reames, D. V. and von Rosenvinge, T. T., 18th International Cosmic Ray Conf., Bangalore, India, Conference Papers 4, 48, 1983.

Schaeffer, O. A. and Zahringer, J., Phys. Rev. Letters 8, 389., 1962.

Van Allan, J. A. and Krimigis, S. M., J. Geophys. Res. 70, 5737, 1965.

von Rosenvinge, T. T., McDonald, F. B., Trainor, J. H., Van Hollebeke, M. A. I., and Fisk, L. A., IEEE Transactions on Geoscience Electronics GE-16., 208, 1978.

FIGURES

Figure 1 A portion of the dE/dx versus E pulse-height matrix for particles stopping in the second 15 micron element of the VLET detector. Numbers on the plot are the number of particles at that position. Tracks of He isotopes, visible by eye, are identified on the plot.

Figure 2 Time histories of the intensities of ^{3}He and electrons of the indicated energy during May 17, 1979. The appearance of the plots differ partly because of the absence of continuous background fluxes for ^{3}He. The lowest isolated points for each energy of ^{3}He represent one particle per 15 minute averaging period. The rapidly varying bursts (at ~ 0400 UT and ~ 1200 UT) observed in the higher, 19 keV, energy electron channels are due to particles from the Earth's bow shock. The 53-104 keV channel also responds to solar X-rays (~ 0130, 1630-2030, and 2330 UT). The dashed vertical line indicates the time of the Type III solar radio burst. Intensity scale factors are shown to the right of the energies.

Figure 3 Time histories of the intensities of ^{3}He and electrons during December 26-27, 1978 (see Figure 2). From ~ 1830-1930 UT, the electron experiment undergoes a calibration cycle.

Figure 4 Time histories of the intensities of ^{3}He and electrons during September 6-7, 1979 (see Figure 2).

Figure 5 Time histories of the intensities of ^{3}He and electrons during November 8-9, 1978 (see Figure 2). Hourly averaged ^{3}He intensities are shown in this event.

Figure 6 Time of onset and peak flux for particles plotted versus $1/\beta$ where $v = \beta c$ is the particle velocity. The lines represent least-squares fits to the electron data only.

Figure 7 Time histories of ^3He and ^4He (15 minute averaged) on May 17, 1979. Ambient ^4He remains from increases on the previous day and does not appear to be associated with the ^3He event.

Figure 8 Helium angular distribution showing the direction of motion of helium particles integrated over the event period when ^3He dominates the rate. Sectoring is relative to the solar direction at the top of the figure. The magnetic field direction and its variation, shown as B, lies near the antisolar direction.

Figure 9 Angular distributions in the directions of motion of electrons at various energies from 2.0 to 8.5 keV. Sectoring is relative to the local magnetic field (unlike Figure 8). The antisolar direction and its variation are indicated near the bottom in each plot.

Figure 10 Event-averaged energy spectra for electrons and ^3He in the May 17, 1979 event. Lines through the data are least-squares fit lines to power-law spectra with resulting spectral indices 2.7 ± 0.1 for electron and 2.7 ± 0.3 for ^3He. The electron fit was confined to the 2.5 to 60 keV region.

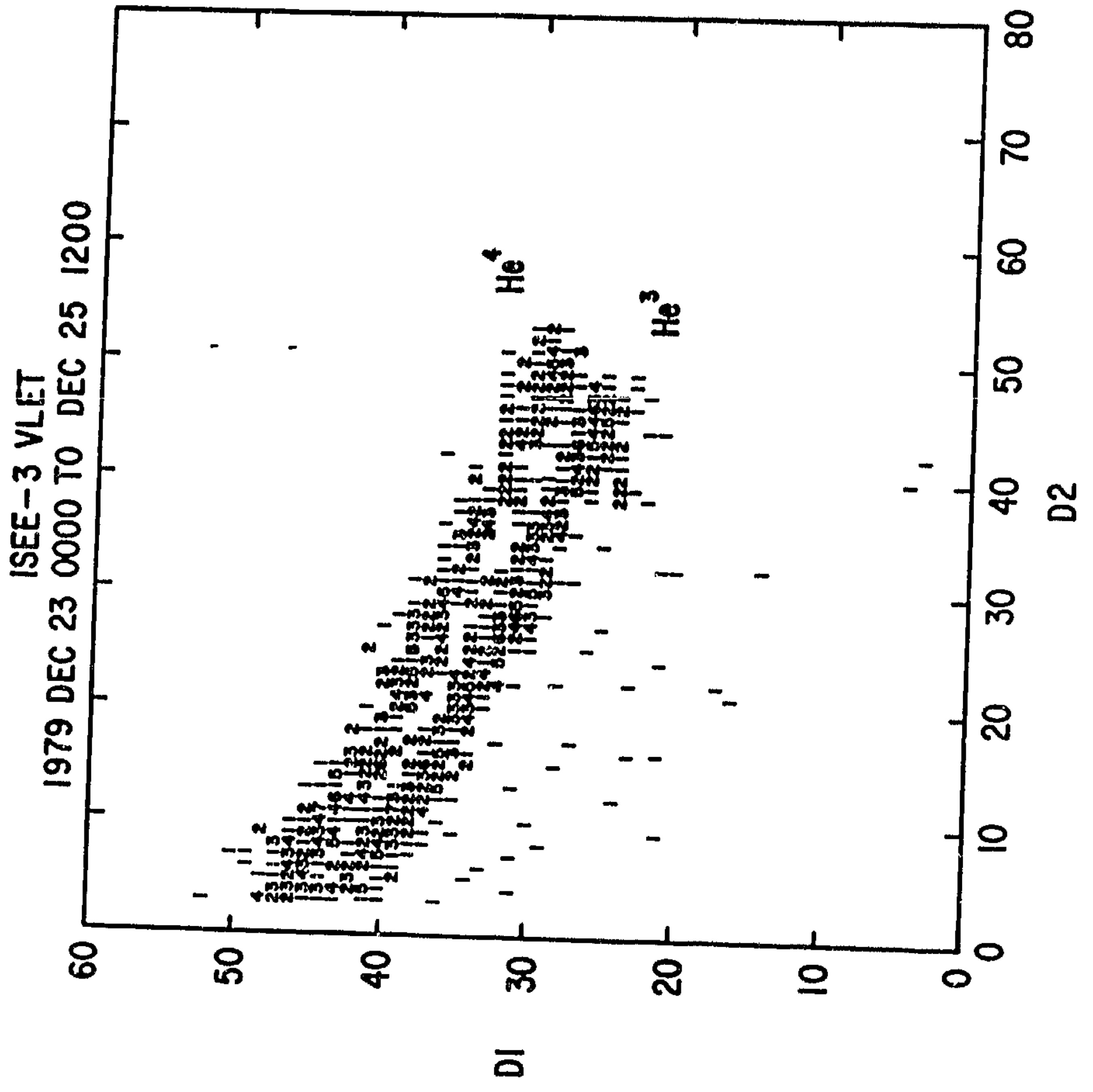
ISEE-3 VLET
1979 DEC 23 0000 TO DEC 25 1200
DI
D2
He4
He3
0
10
20
30
40
50
60
70
80

Figure 1

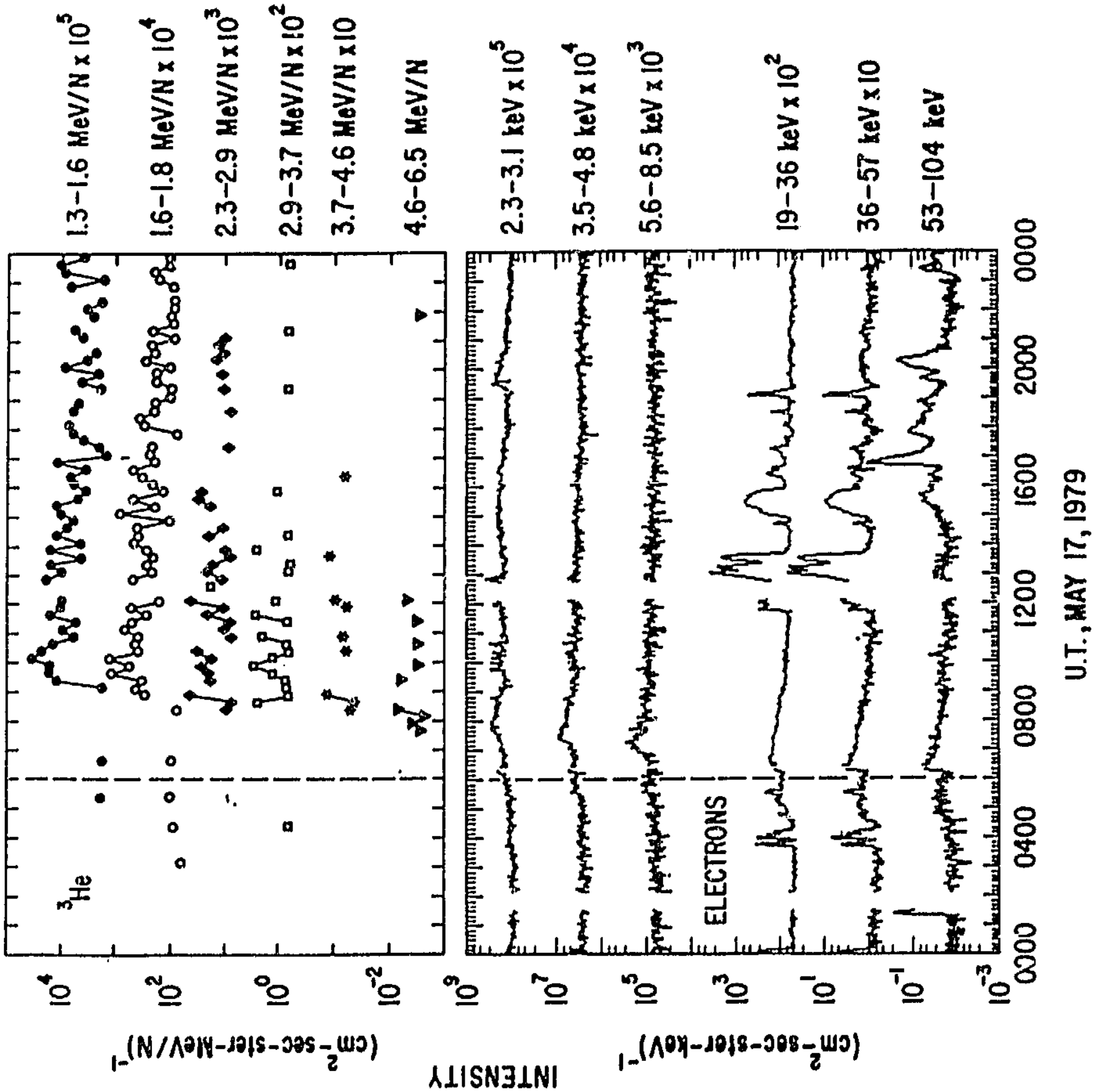

^3He
1.3–1.6 MeV/N x 10^5
1.6–1.8 MeV/N x 10^4
2.3–2.9 MeV/N x 10^3
2.9–3.7 MeV/N x 10^2
3.7–4.6 MeV/N x 10
4.6–6.5 MeV/N
ELECTRONS
2.3–3.1 keV x 10^5
3.5–4.8 keV x 10^4
5.6–8.5 keV x 10^3
19–36 keV x 10^2
36–57 keV x 10
53–104 keV
INTENSITY
$(cm^2\text{-sec-ster-MeV/N})^{-1}$
$(cm^2\text{-sec-ster-keV})^{-1}$
U.T., MAY 17, 1979

Figure 2

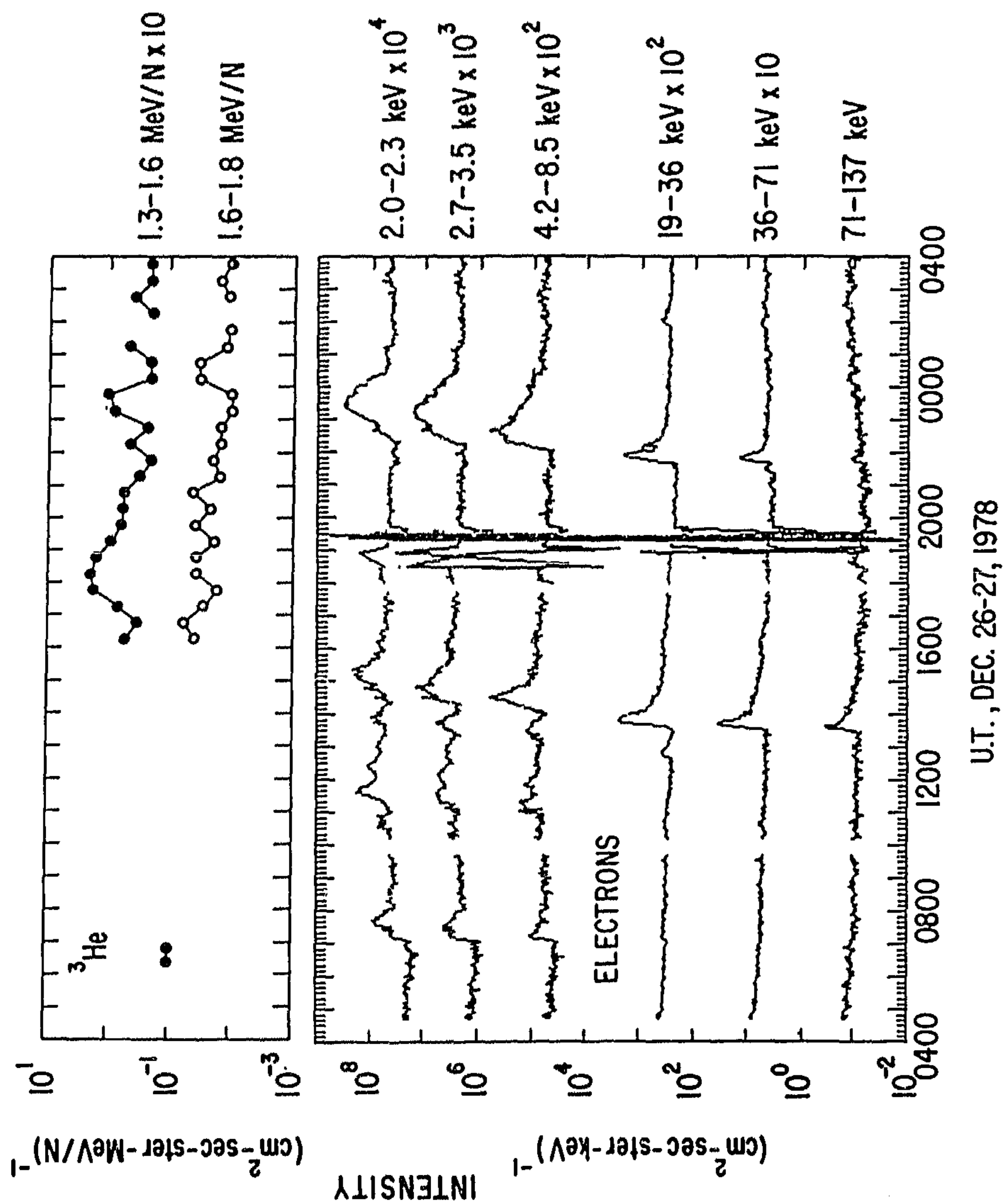

1.3–1.6 MeV/N x 10
1.6–1.8 MeV/N
2.0–2.3 keV x 10^4
2.7–3.5 keV x 10^3
4.2–8.5 keV x 10^2
19–36 keV x 10^2
36–71 keV x 10
71–137 keV
3He
ELECTRONS
INTENSITY
(cm2-sec-ster-MeV/N)-1
(cm2-sec-ster-keV)-1
U.T., DEC. 26-27, 1978
0400
0800
1200
1600
2000
0000
0400

Figure 3

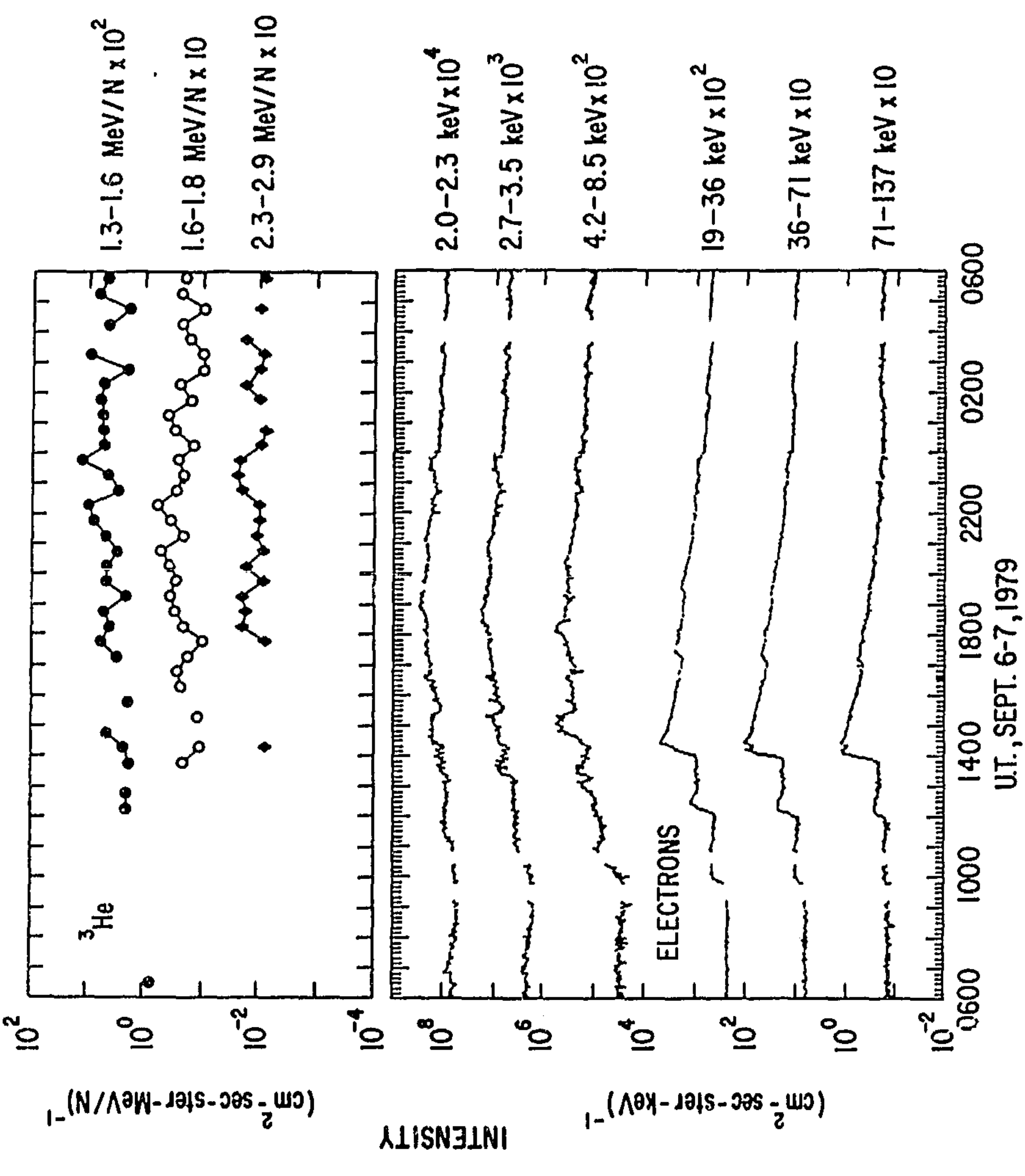

1.3–1.6 MeV/N x 10^2
1.6–1.8 MeV/N x 10
2.3–2.9 MeV/N x 10
2.0–2.3 keV x 10^4
2.7–3.5 keV x 10^3
4.2–8.5 keV x 10^2
19–36 keV x 10^2
36–71 keV x 10
71–137 keV x 10
3He
ELECTRONS
INTENSITY
(cm^2-sec-ster-MeV/N)^-1
(cm^2-sec-ster-keV)^-1
U.T., SEPT. 6-7, 1979
0600
1000
1400
1800
2200
0200
0600

Figure 4

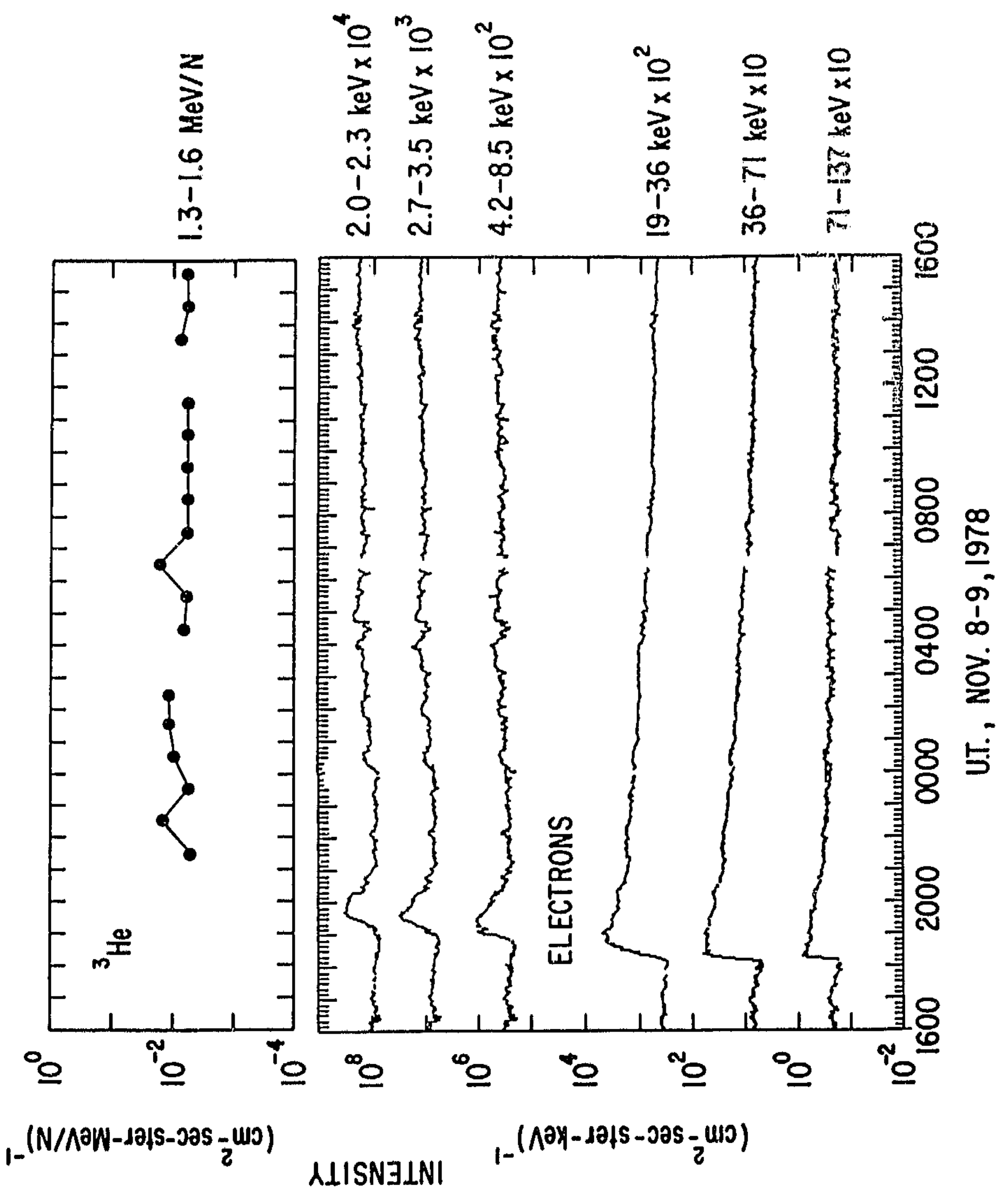

1.3–1.6 MeV/N
^3He
2.0–2.3 keV x 10^4
2.7–3.5 keV x 10^3
4.2–8.5 keV x 10^2
ELECTRONS
19–36 keV x 10^2
36–71 keV x 10
71–137 keV x 10
INTENSITY
(cm^2-sec-ster-MeV/N)$^{-1}$
(cm^2-sec-ster-keV)$^{-1}$
U.T., NOV. 8-9, 1978
1600
2000
0000
0400
0800
1200
1600
10^0
10^{-2}
10^{-4}
10^8
10^6
10^4
10^2
10^0
10^{-2}

Figure 5

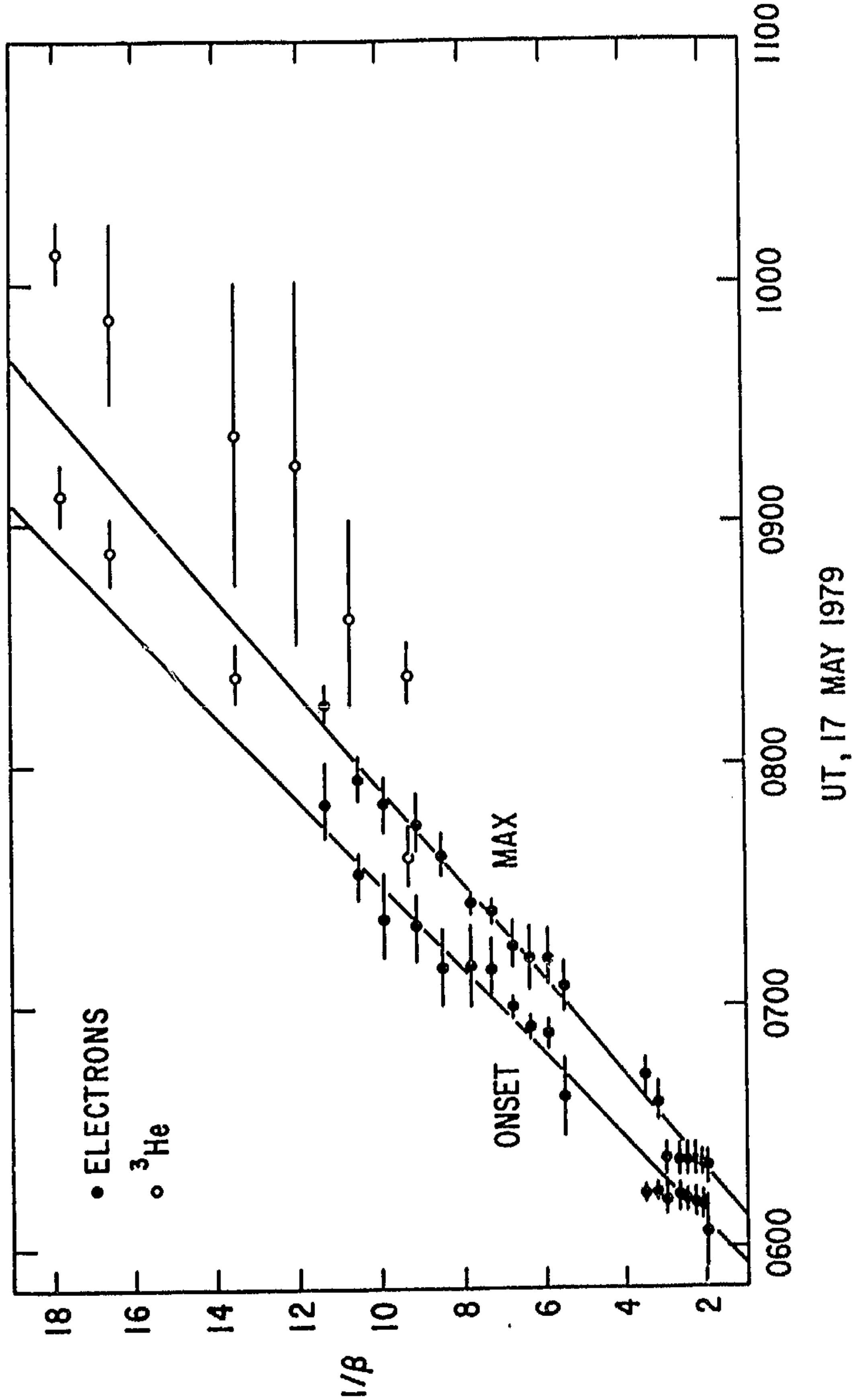

• ELECTRONS
∘ ³He
ONSET
MAX
1/β
UT, 17 MAY 1979
0600
0700
0800
0900
1000
1100
2
4
6
8
10
12
14
16
18

Figure 6

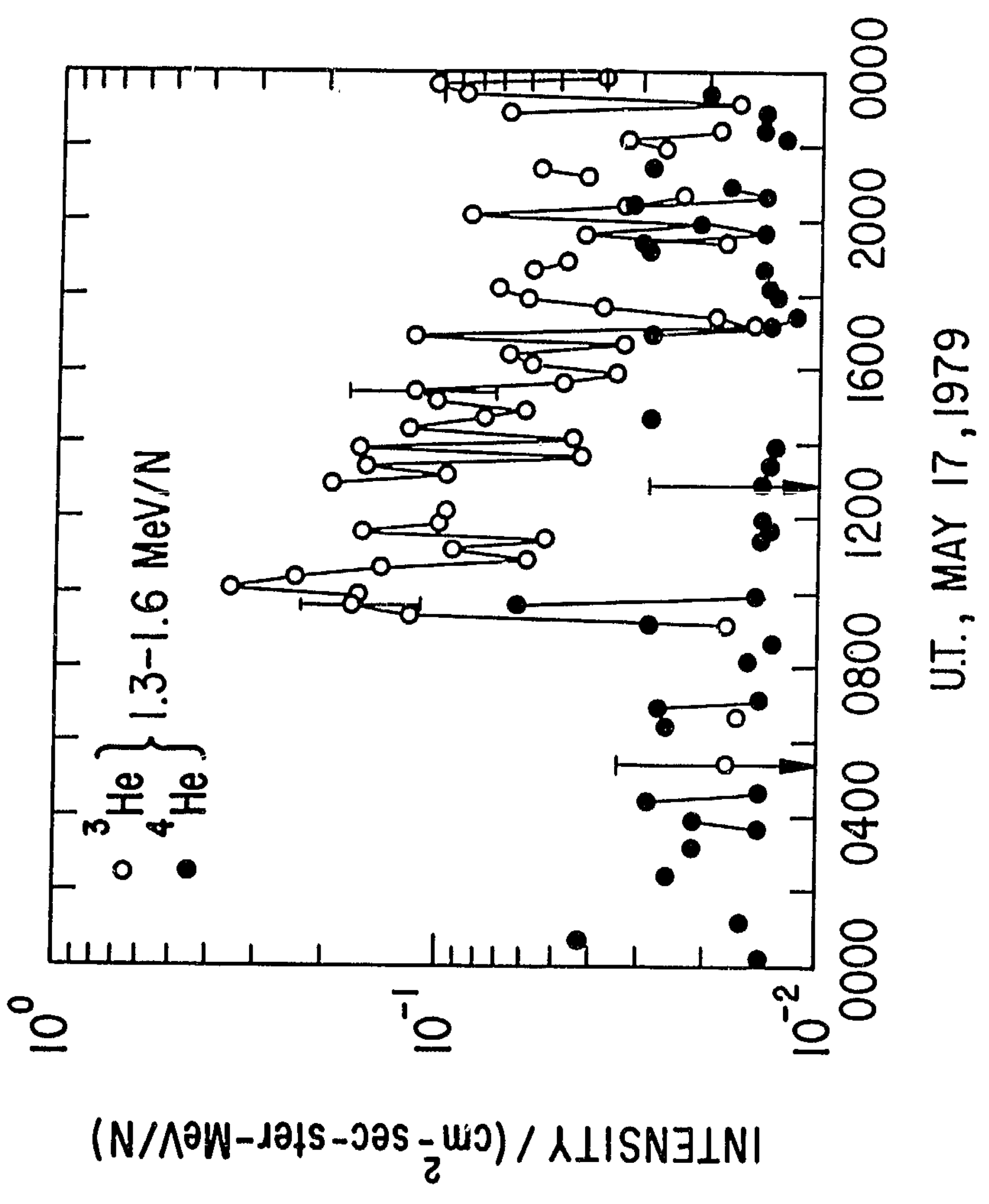

INTENSITY / (cm²-sec-ster-MeV/N)
10⁰
10⁻¹
10⁻²
³He
⁴He
1.3-1.6 MeV/N
0000
0400
0800
1200
1600
2000
0000
U.T., MAY 17, 1979

Figure 7

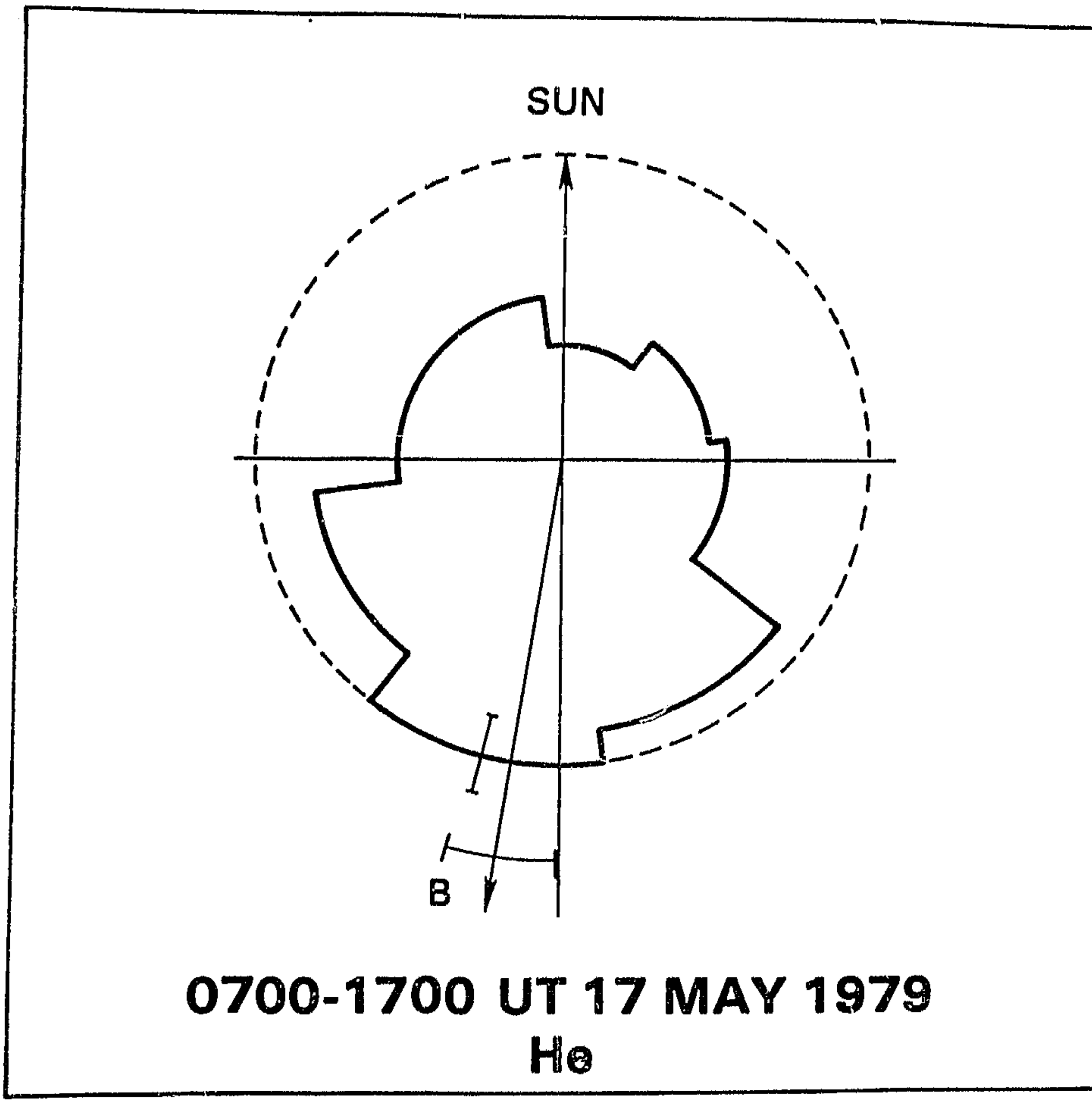

Figure 8

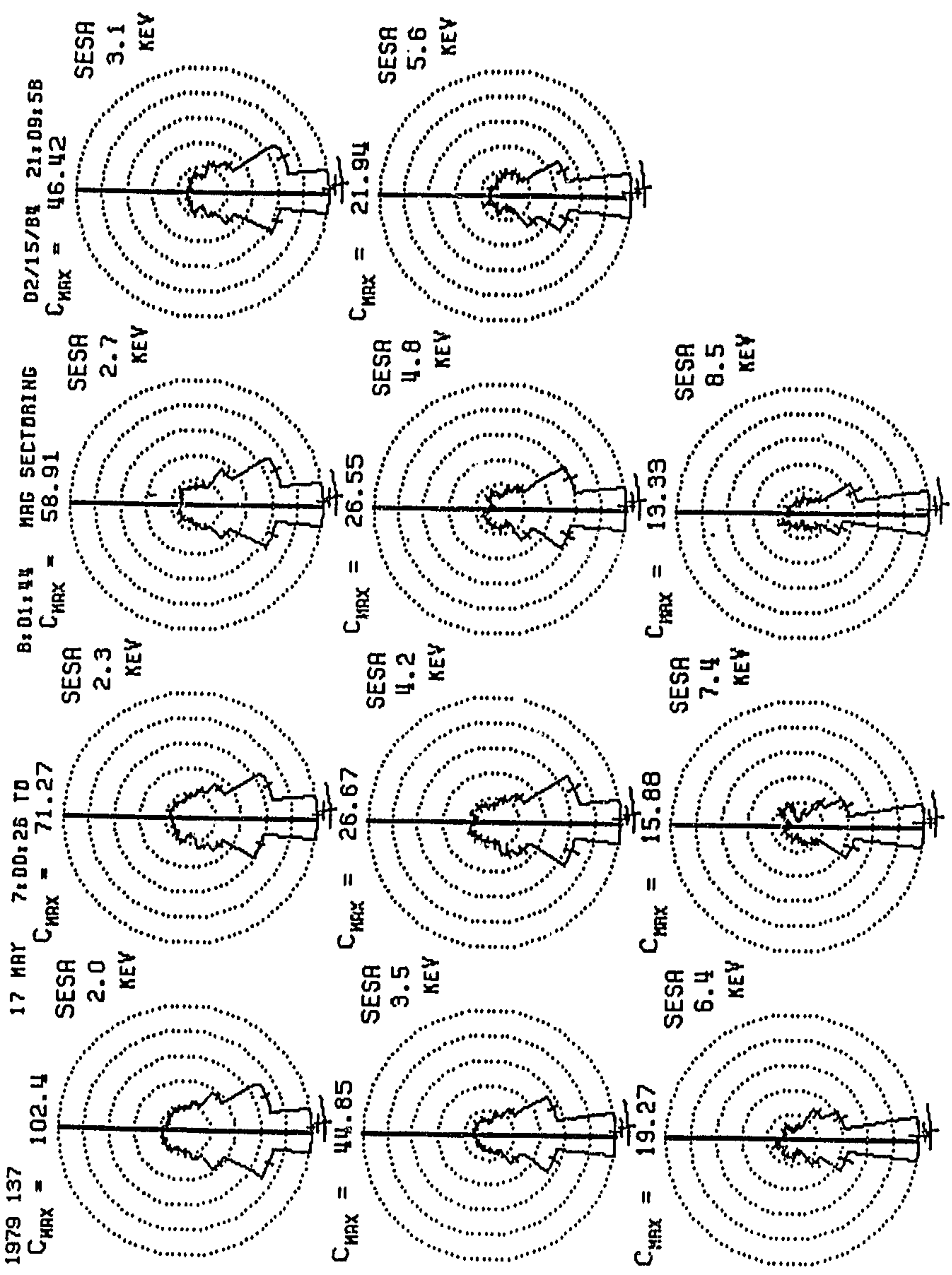

1979 137
17 MAY 7:00:26 TO
MAG SECTORING
21:09:58
CMAX = 102.4
CMAX = 71.27
CMAX = 58.91
CMAX = 46.42
CMAX = 44.85
CMAX = 26.67
CMAX = 26.55
CMAX = 21.94
CMAX = 19.27
CMAX = 15.88
CMAX = 13.33
SESA 2.0 KEV
SESA 2.3 KEV
SESA 2.7 KEV
SESA 3.1 KEV
SESA 3.5 KEV
SESA 4.2 KEV
SESA 4.8 KEV
SESA 5.6 KEV
SESA 6.4 KEV
SESA 7.4 KEV
SESA 8.5 KEV

Figure 9

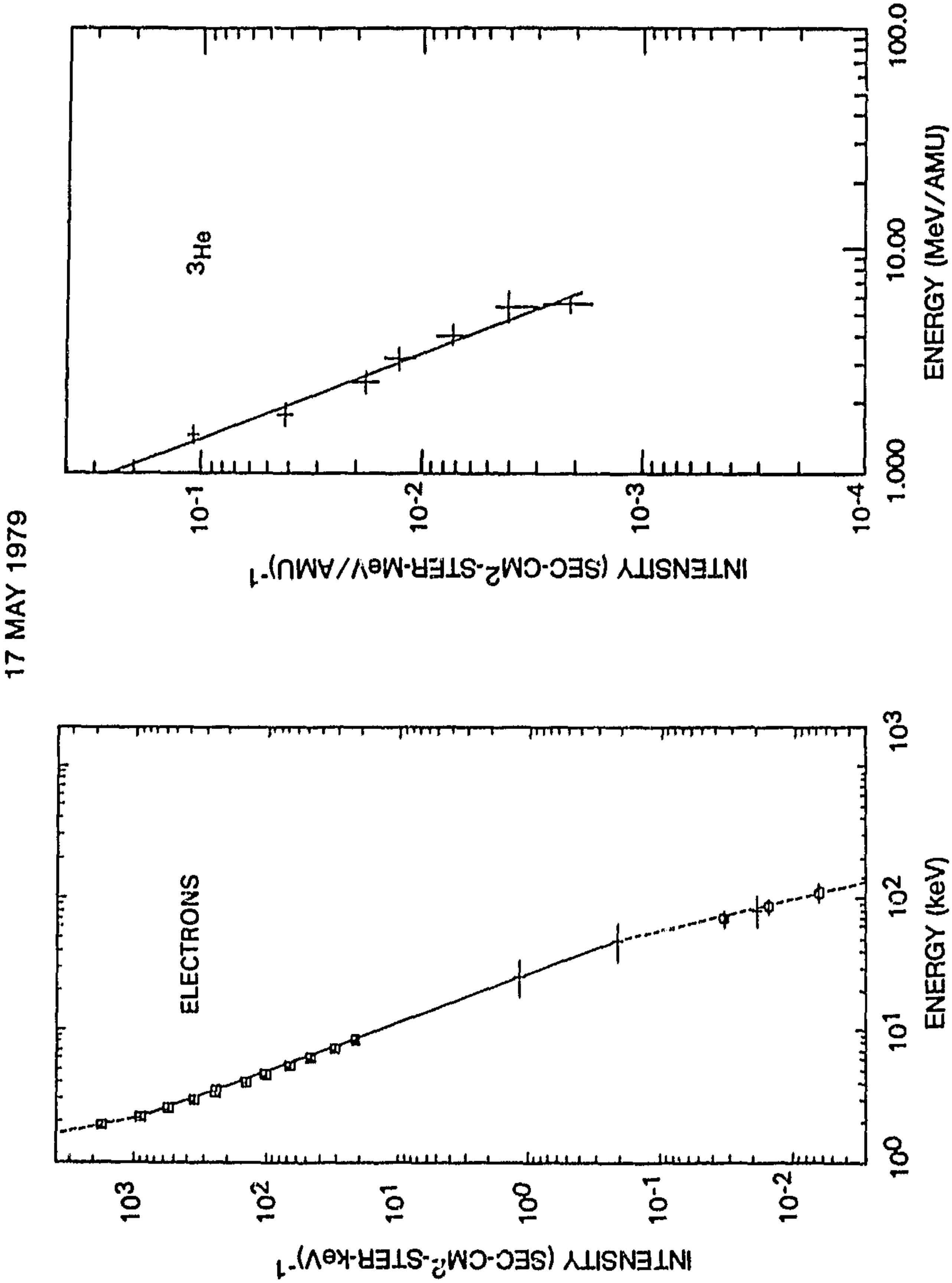

17 MAY 1979
ELECTRONS
ENERGY (keV)
INTENSITY (SEC-CM2-STER-keV)-1
3He
ENERGY (MeV/AMU)
INTENSITY (SEC-CM2-STER-MeV/AMU)-1

Figure 10